Creep Analysis of FGM Cylinder In The Presence Of Residual Stress

Mr. Kulkarni Vyankatesh Shrikant

Research Scholar, CMJ University, Shillong, Meghalaya, India

Abstract – The study reported in this paper puts forward a framework for the analysis of steady state creep behaviour of a thick-walled cylinder made of FGM in the presence of thermal residual stress. The problem undertaken has significant practical importance. In order to describe yielding of FGM in the presence of thermal residual stress, the Hoffman"s yield criterion is used.

----------♦----------

6.1 GENERAL

Residual stress originates in metal matrix composites during processing, involving cooling from high temperature to room temperature. The presence of residual stress results in difference of yield stress of composite in tension and compression. The von-Mises yield criterion for isotropic material assumes that yielding under both uniaxial tension and compression starts at the same level of stress.

However, the experimental results (Arsenault, 1987) often indicate that even in isotropic metal matrix composite yielding does not begins at the same level of tensile and compressive stresses under uniaxial loading. These composites are generally reinforced with ceramic materials having relatively lower coefficient of thermal expansion as compared to the matrix phase. During processing when these composites are cooled from a higher temperature, the thermal residual tensile stresses are induced in the matrix due to restraint imposed by the ceramic reinforcements. A part of the matrix residual stress is relaxed by plastic deformation, thereby, increasing the density of matrix dislocation, which contributes in strengthening of the composite.

The study reported in this chapter puts forward a framework for the analysis of steady state creep behaviour of a thick-walled cylinder made of FGM in the presence of thermal residual stress. The problem undertaken has significant practical importance. In order to describe yielding of FGM in the presence of thermal residual stress, the Hoffman"s yield criterion is used.

6.2 DISTRIBUTION OF REINFORCEMENT AND ESTIMATION OF CREEP PARAMETERS

The FGM cylinder taken in this study is assumed to be made of 6061Al- SiCw composite. The amount of SiCw in the FGM cylinder is assumed to decrease linearly from the inner (*a)* to outer radius (*b)*. The content of silicon carbide *V(r)* at any radius *r* of the cylinder is again estimated from Eqn. 4.1. The average and minimum whisker contents in the cylinder are estimated respectively from Eqs. 4.4 and 4.5.

The creep parameters *M(r)* and o (*r*) , required for estimating the distribution of stresses and strain rates in the FGM cylinder, are computed respectively from regression Eqs. (5.3) and (5.4) developed in chapter 5. These equations are rewritten as below,

$$M = 0.02876 - \frac{0.00879}{P} - \frac{14.02666}{T} + \frac{0.03224}{V(r)} + dM_1 + dM_2 \qquad (6.1)$$

$$\sigma_o = -0.084P - 0.0232T + 1.1853(V(r)) + 22.207 + d\sigma_{o_1} + d\sigma_{o_2} \qquad (6.2)$$

In this study, the FGM cylinder is assumed to operate at a constant temperature (288 *oC*) and size of SiCw is kept constant (=1.23 *μm*). Therefore, the creep parameters *M* and *o* will be functions of only radial distance *r*, due to radially varying amount of SiCw in the FGM cylinder.

6.3 ANALYSIS OF CREEP IN FGM CYLINDER

The analysis of steady state creep in thick-walled functionally graded cylinder may proceed in a similar fashion as described in chapter 4 for isotropic FGM

cylinder. However, in this study the reinforcements are assumed to be in whiskers form rather than particle shape, whereas the matrix is chosen as 6061Al instead of pure aluminum. The assumptions made for the purpose of analysis are similar to those described in section 4.5 (chapter 4) for isotropic FGM cylinder. The FGM cylinder is subjected to internal pressure (*p*) and zero external pressure.

As described earlier, the deformation compatibility equation for a thick- walled cylinder is,

$$r\frac{d\dot{\varepsilon}_\theta}{dr} = \dot{\varepsilon}_r - \dot{\varepsilon}_\theta \tag{6.3}$$

The following boundary conditions are used in this analysis,

$$\text{At} \quad r = a \qquad \sigma_r = -p \tag{6.4}$$

$$\text{At} \quad r = b \qquad \sigma_r = 0 \tag{6.5}$$

where the negative sign implies compressive nature of radial stress.

The equilibrium equation for the cylinder is,

$$r\frac{d\sigma_r}{dr} = \sigma_\theta - \sigma_r \tag{6.6}$$

Hoffman‟s yield criterion for isotropic materials is capable of taking into account the difference in yield strength under tension and compression, which differ significantly in a metal matrix composite depending on its processing route. As suggested by several investigators (Pankaj *et al*, 1999; Bicanic *et al*, 1994), the Hoffman‟s isotropic yield criterion for a material having different yield strength in tension and compression may be expressed as,

$$(\sigma_{11}^2+\sigma_{22}^2+\sigma_{33}^2)-(\sigma_{11}\sigma_{22}+\sigma_{22}\sigma_{33}+\sigma_{33}\sigma_{11}) + (f_c-f_t)(\sigma_{11}+\sigma_{22}+\sigma_{33}) - f_c f_t = 0 \tag{6.6}$$

where *f c* and *f t* are respectively the uniaxial compressive and tensile yield strength of the material. The yield criterion given above may also be written as,

$$\frac{1}{2f_c f_t}\left[(\sigma_{22}-\sigma_{33})^2+(\sigma_{33}-\sigma_{11})^2+(\sigma_{11}-\sigma_{22})^2\right]+\frac{(f_c-f_t)}{f_c f_t}(\sigma_{11}+\sigma_{22}+\sigma_{33})=1 \tag{6.7}$$

The associated flow rule given in Eqn. (3.12) is,

$$d\varepsilon_{ij} = \frac{\partial f}{\partial \sigma_{ij}}d\lambda \tag{6.8}$$

As described in chapter 3 [Eqn. (3.16)], the effective stress and effective strain are related as,

$$d\varepsilon_e = \sigma_e d\lambda \tag{6.9}$$

Using the flow rule given in Eqn. (6.8) into the yield criterion given by Eqn. (6.7), we get the following set of constitutive equations,

$$\left\{\begin{array}{l} \dot{\varepsilon}_{11} = \dfrac{\dot{\varepsilon}_e}{2\sigma_e}[(\sigma_{11}-\sigma_{33})+(\sigma_{11}-\sigma_{22})+(f_c-f_t)] \\ \dot{\varepsilon}_{22} = \dfrac{\dot{\varepsilon}_e}{2\sigma_e}[(\sigma_{22}-\sigma_{33})+(\sigma_{22}-\sigma_{11})+(f_c-f_t)] \\ \dot{\varepsilon}_{33} = \dfrac{\dot{\varepsilon}_e}{2\sigma_e}[(\sigma_{33}-\sigma_{22})+(\sigma_{33}-\sigma_{11})+(f_c-f_t)] \end{array}\right\} \tag{6.10}$$

If the principal directions 1, 2 and 3 are taken respectively along *r*, *θ* and *z* directions of the FGM cylinder, the above set of equations become,

$$\dot{\varepsilon}_r = \frac{d\dot{u}_r}{dr} = \frac{\dot{\varepsilon}_e}{2\sigma_e}[2x-1-y+J]\sigma_\theta \tag{6.11}$$

$$\dot{\varepsilon}_\theta = \frac{\dot{u}_r}{r} = \frac{\dot{\varepsilon}_e}{2\sigma_e}[2-y-x+J]\sigma_\theta \tag{6.12}$$

$$\dot{\varepsilon}_z = \frac{\dot{\varepsilon}_e}{2\sigma_e}[2y-x-1+J]\sigma_\theta \tag{6.13}$$

Where

$x=\frac{\sigma_r}{\sigma_\theta}$, $y=\frac{\sigma_z}{\sigma_\theta}$, $J=\frac{f_c-f_t}{\sigma_\theta}$, $\dot{\varepsilon}_e$ is the effective strain rate and is the effective stress.

The values of *f c* and *f t* for 6061Al-SiCw composite are taken from the experimental results reported by Badini (1990). Badini (1990) observed that for extruded bars made of 6061Al matrix composite reinforced with SiCw, the

yield strength *f c* and *f t* are respectively 218 *MPa* and 186 *MPa*.

According to Hoffman"s yield criterion, the effective stress (e) in an isotropic cylinder is given by,

$$\sigma_e = \sigma_\theta[1 + x^2 + y^2 - x - y - xy + J(1 + x + y)]^{1/2} \quad (6.14)$$

Under plane strain condition (*i.e.* z 0), Eqn. (6.13) gives,

$$\sigma_z = \frac{\sigma_r + \sigma_\theta - (f_c - f_t)}{2} \quad (6.15)$$

Dividing Eqn. (6.11) by Eqn. (6.12), we get,

$$\frac{d\dot{u}}{dr}\frac{r}{\dot{u}_r} = \varphi(r) \quad (6.16)$$

$$\text{where, } \varphi(r) = \frac{2x - 1 - y + J}{2 - y - x + J}$$

Integrating Eqn. (6.16) from *a* to *r*, we obtain,

$$\dot{u}_r = \dot{u}_a\left[\exp\int_a^r \frac{\varphi(r)}{r}\,dr\right] \quad (6.17)$$

where *u a* is radial displacement at the internal radius of FGM cylinder.

Dividing Eqn. (6.17) by *r* and equating it to Eqn. (6.12), we get,

$$\frac{\dot{u}_r}{r} = \dot{\varepsilon}_\theta = \frac{\dot{\varepsilon}_e}{2\sigma_e}[2 - y - x + J]\sigma_\theta = \frac{\dot{u}_a}{r}\left[\exp\int_a^r \frac{\varphi(r)}{r}\,dr\right] \quad (6.18)$$

Substituting *e* from Eqn. (3.2) and *e* from Eqn. (6.14) into Eqn. (6.18) and simplifying, we get;

$$\sigma_\theta = \frac{(\dot{u}_a)^{1/n}}{M} I_1(r) + I_2(r) \quad (6.19)$$

where,

$$I_1(r) = \left[\frac{2(x^2 + y^2 - x - y - xy + J(1 + x + y))^{\frac{1-n}{2}}}{r[2 - y - x + J]}\left\{\exp\int_a^r \frac{\varphi(r)}{r}\,dr\right\}\right]^{1/n}$$

and,

$$I_2(r) = \frac{\sigma_o}{\sqrt{x^2 + y^2 - x - y - xy + J(1 + x + y)}}$$

Integrating equilibrium Eqn. (6.6) between limits „*a*" to „*b*", and using the boundary conditions given in Eqs. (6.4) and (6.5), we get,

$$\int_a^b \sigma_\theta dr = ap \quad (6.20)$$

Substituting from Eqn. (6.19) into above equation and simplifying, we obtain,

$$\frac{(\dot{u}_a)^{1/n}}{M} = \frac{ap}{\int_a^b I_1 dr} - \frac{\int_a^b I_2(r)dr}{\int_a^b I_1(r)} \quad (6.21)$$

Using Eqn. (6.21) into Eqn. (6.19), we get

$$\sigma_\theta = \left[\frac{ap}{\int_a^b I_1(r)dr} - \frac{\int_a^b I_2(r)dr}{\int_a^b I_1(r)dr}\right] I_1(r) + I_2(r) \quad (6.22)$$

The average tangential stress in the FGM cylinder may be obtained from Eqn. (6.20) by dividing both sides by (*b* - *a*) as,

$$\sigma_{\theta avg} = \frac{ap}{b - a} \quad (6.23)$$

Substituting the value of *ap* from Eqn. (6.23) into Eqn. (6.22), we get,

$$\sigma_\theta = \left[\frac{(b - a)\sigma_{\theta avg}}{\int_a^b I_1(r)dr} - \frac{\int_a^b I_2(r)dr}{\int_a^b I_1(r)dr}\right] I_1(r) + I_2(r) \quad (6.24)$$

Integrating equilibrium Eqn. (6.6) once again between limit *a* to *r*, we obtain,

$$\sigma_r = \frac{1}{r}\int_a^r \sigma_\theta dr - \frac{ap}{r} \quad (6.25)$$

Using Eqs. (6.14) and (6.15) in Eqs. (6.11) and (6.12), we may get the following relationship between effective (□□e), tangential (□□□) and radial (□□r) strain rates,

$$\dot{\varepsilon}_\theta = -\dot{\varepsilon}_r = 0.87\dot{\varepsilon}_e \frac{[1-x+J]}{\left[1+x^2-2x+\frac{J^2}{3}+2J+2xJ\right]^{1/2}} \qquad (6.26)$$

In case of FGM cylinder without residual stress (J = 0), the above equation reduces to,

$$\dot{\varepsilon}_\theta = -\dot{\varepsilon}_r = 0.87\dot{\varepsilon}_e \qquad (6.27)$$

The above equation is similar to that obtained earlier in chapter 4 (Eqn. 4.18).

6.4 NUMERICAL COMPUTATIONS

The stresses and strain rates in the FGM cylinder are obtained by an iterative scheme of computation, as described below. In order to find the first approximation of x and y *i.e.* $x1$ and $y1$, we assume in Eqn. (6.25) and solving, we get the first approximation of □ r (*i.e.*□ r) as,

$$\sigma_{r_1} = \frac{ap}{r}\left[\frac{r-b}{b-a}\right] \qquad (6.28)$$

Therefore, $x_1 = \frac{\sigma_{r_1}}{\sigma_{\theta avg}} = 1-\frac{b}{r}$

where $\sigma_{z_1} = \frac{\sigma_{r_1}+\sigma_{\theta avg}-(f_c-f_t)}{2}$ as obtained from Eqn. (6.15).

The values of $x1$ and $y1$, thus obtained, are used to get first approximations of $I1(r)$, $I2(r)$ and $\varphi(r)$, which are substituted in Eqn. (6.19) to get first approximation of σ_θ $(i.e.\ \sigma_{\theta_1})$.

Using $\sigma_\theta = \sigma_{\theta_1}$ again in Eqn. (6.25), we may get the second approximation of □ r *i.e.* □ . Following procedure described above, one may get 2 the second approximations of $I1(r)$, $I2(r)$ and $\varphi(r)$ and hence may find second approximation of □□ (*i.e.* □ □). The process is continues, till the difference between the values of □□ estimated in the current and previous steps becomes less than 0.01, over the entire radius of cylinder. Thereafter, one may estimate the final values of □ r and □ z respectively from Eqs. (6.25) and (6.15).

Knowing the distributions of □ r , □ □ and □ z , we may estimate □ e and □□e respectively from Eqs. (6.14) and (3.2). Thereafter, the strain rates □□r , □□□ and □□z in the FGM cylinder are calculated respectively from Eqs. (6.11), (6.12) and (6.13).

6.5 RESULTS AND DISCUSSION

6.5.1 Validation

Before discussing the results obtained through current analytical scheme, it is necessary to check the validity of analysis as well as software developed for the purpose of computations. For this purpose, the current analysis and software developed is used to obtain the tangential strain rates in an isotropic copper cylinder, as reported in the study of Johnson *et al* (1961). The procedure for obtaining the results is described in section 5.6.1. The tangential strain rates estimated agree well with the experimental values reported by Johnson *et al* (1961), similar to those observed in Fig. 5.2.

6.5.2 Distribution[1] of Creep Stresses and Creep Rates

The steady state creep stresses and creep rates have been obtained for FGM cylinder made of 6061Al-SiCw having thermal residual stress (*f c* - *f t*) =32 *MPa*, as derived from the experimental results reported by Badini (1990). These results have been compared with those obtained for a similar FGM cylinder but without residual stress *i.e. f c* □ *f t* .

The FGM cylinder chosen in this study is assumed to contain a maximum of 15 *vol%* SiCw at the inner radius and an average of 10 *vol%* SiCw. The content *V(r)* of SiCw in the FGM cylinder decreases linearly from the inner to outer radius, as shown in Fig. 6.1. The cylinder is subjected to an internal pressure (p) = 85.25 *MPa* and zero external pressure. The dimensions of the cylinder used in this study are kept similar to those reported in the study of Johnson *et al* (1961) for copper cylinder (refer Table 3.2).

Figures 6.2(a)-(b) show the variation of creep parameters *M(r)* and □ o (*r*) with radial distance in the FGM cylinders. The values of creep parameters in both the cylinders are equal. Further, the value of creep parameter *M* increases with increasing radial distance, Fig. 6.2(a). The increase observed in *M* may be attributed to decrease in particle content *V(r)*, on moving from the inner to outer radius of the cylinder. On the other hand, the threshold stress (□ o) shown in Fig. 6.2(b) decreases linearly on moving from the inner to outer radius of the FGM cylinders. The threshold stress is higher in locations having more amount of SiCw reinforcement as compared to locations having lower SiCw content.

The radial stress, Fig. 6.3(a), remains compressive throughout the cylinder, with maximum value at the inner radius and zero at the outer radius, under the imposed boundary conditions given in Eqs. (6.4) and (6.5). In the presence of residual stress, the magnitude of radial stress in the FGM cylinder changes a little. In the middle of cylinder, the radial stress in FGM cylinder C2 is slightly lower than those observed in FGM cylinder C1 without residual stress. The tangential stress in FGM cylinder C1 remains tensile throughout and is observed to increase with increasing radius, reaches maximum (70.04 *MPa*) at a radius of 46.56 *mm*, followed by a decrease towards the outer radius, Fig. 6.3(b). If the yield plasticity follows the Hoffman"s yield criterion, it is observed that the tangential stress in the FGM cylinder C2 increases near the inner radius but decreases towards the outer radius when compared with FGM cylinder C1. The maximum increase and decrease observed in tangential stress respectively at the inner and outer radii are 6.84 *MPa* and 5.41 *MPa*. The presence of residual stress leads to a slight shift in the location of maximum tangential stress towards the inner radius and it also decrease the magnitude of maximum tangential stress by 4.06 *MPa*.

The axial stress changes its nature from compressive to tensile on moving from the inner to outer radius of the FGM cylinders, Fig. 6.3(c). The presence of residual stress in FGM cylinder decreases the magnitude of tensile axial stress (observed near the outer radius) but increases the compressive stress (observed near the inner radius). In the presence of residual stress, the compressive value of axial stress increases by 12.58 *MPa* at the inner radius whereas the tensile value of axial stress, observed at outer radius, decreases by 17.2 *MPa*.

The effective stress, Fig. 6.3(d), decreases with increasing radial distance. In the presence of residual stress, the effective stress at the inner radius decreases a little but exhibits a significant increase towards the outer radius. The effective stress observed in FGM cylinder C2 exhibits a cross over at a radius of 26.93 *mm*. Inspite of similar distribution of SiCw in FGM cylinders C1 and C2, the effective stress increases significantly in FGM cylinder C2 with residual stress as compared to FGM cylinder C1 without residual stress. The increase observed in effective stress increases with increase in radial distance, except for some portions near the inner radius of the cylinder. The maximum increase observed in effective stress is 13.77 *MPa* at the outer radius.

The variation of strain rates, is dependent on the variation of effective strain rate (□□*e*), which is function of stress difference (□ *e* □ □ o) , as revealed from creep law, Eqn. (3.2). Therefore, to investigate the effect of residual stress on creep rates, the distribution of (□ *e* □ □ o) is plotted in Fig. 6.4. The stress difference (□ *e* □ □ o) observed in FGM cylinder C1 is relatively lower than the FGM cylinder C2, similar to that observed in Fig. 6.3(d) for effective stress. Since the value of (□ *e* □ □ o) is higher near the outer radius of FGM cylinder C2 as compared to FGM cylinder C1, therefore, the effective strain rates in FGM cylinder C2 increases significantly on moving towards the outer radius than that observed in FGM cylinder C1. But near the inner radius, the effective strain rate in FGM cylinder C2 are slightly lower than the FGM cylinder C1 owing to lower stress difference (□ *e* □ □ o) in FGM cylinder C2 than cylinder C1, Fig. 6.4.

Unlike FGM cylinder (C1) without residual stress, the FGM cylinder C2 with residual stress exhibits minima in the effective strain rate almost in the middle of cylinder. The radial and tangential strain rates estimated from Eqn. (6.26) for FGM cylinder C2 with residual stress are always higher than the FGM cylinder C1 without residual stress, Fig. 6.5. The extent of variation observed increases with increase in radial distance. The maximum variation in tangential/radial strain rate is observed at the outer radius. Similar to effective strain rate shown in Fig. 6.5(a), the tangential/radial strain rate also exhibits a minima in the middle of the FGM cylinder C2 with residual stress.

It is evident from the above discussion that the presence of residual stress in the FGM cylinder increases the magnitude of strain rates, which may enhance the chances of distortion in the FGM cylinder.

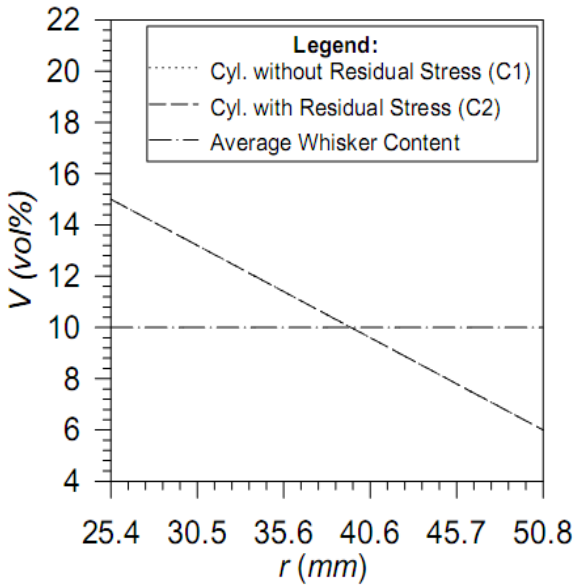

Fig. 6.1: Variation of whisker content in composite cylinders.

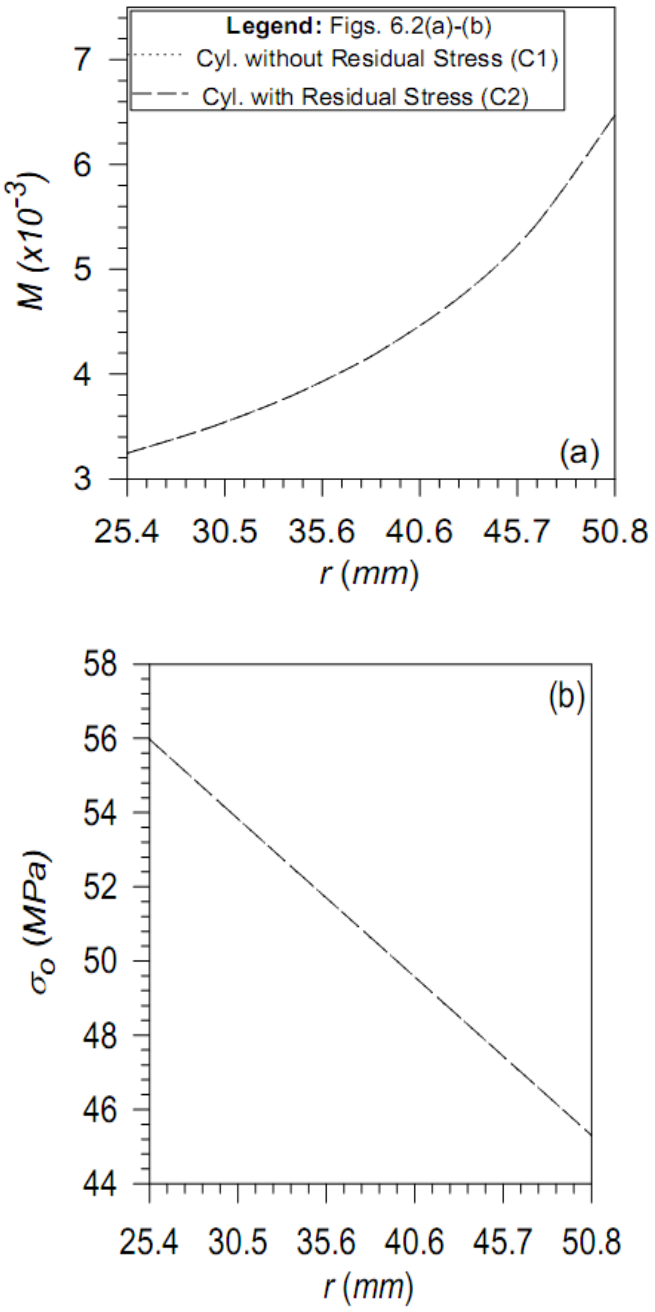

Fig. 6.2: Variation of creep parameters in FGM cylinders.

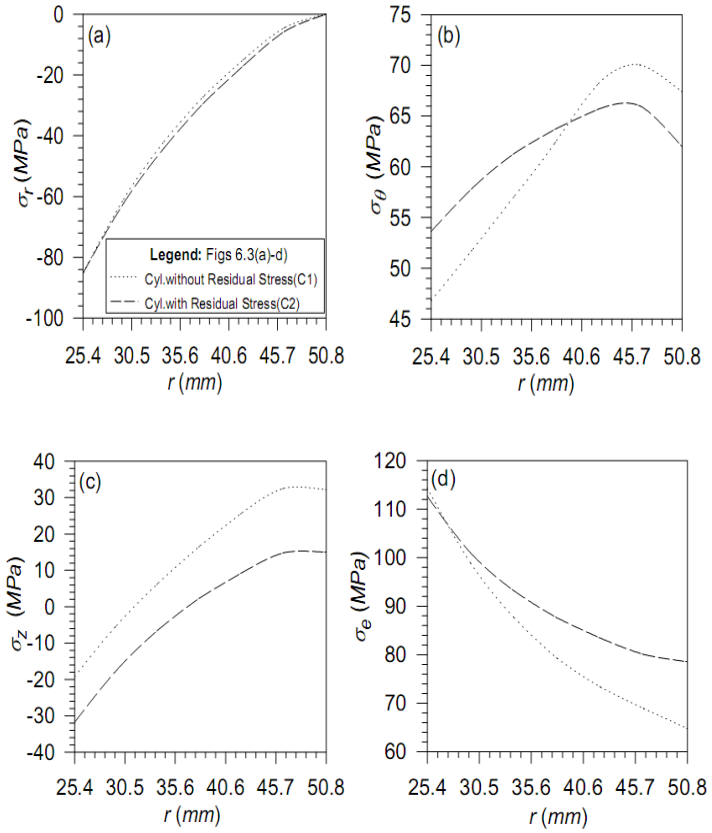

Fig. 6.3: Variation of stresses in different FGM cylinders ($T = 288\ ^{o}C$, $V_{avg} = 10$ *vol%*).

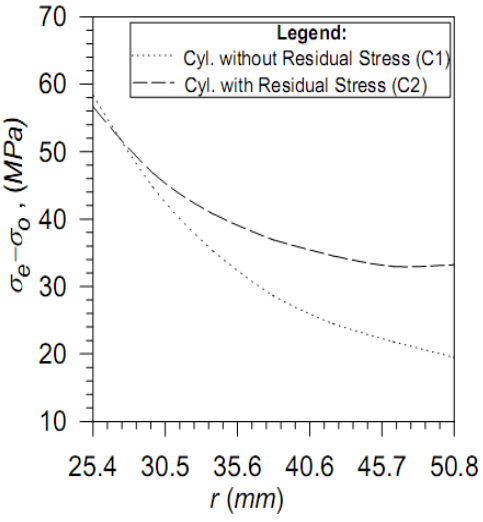

Fig. 6.4: Variation of stress difference in FGM cylinders (T= 288 °C, V_{avg}= 10

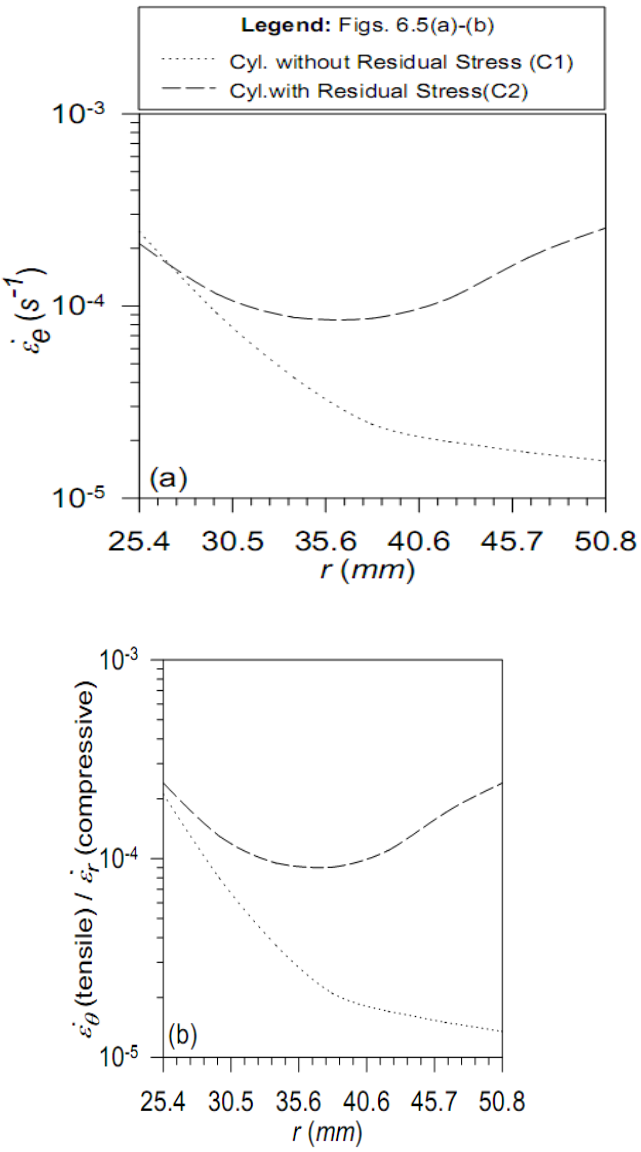

Fig. 6.5: Variation of strain rates in FGM cylinders ($T = 288°C$, $V_{avg} = 10$ *vol%*).

BIBLIOGRAPHY

Abrinia, K., Naee, H., Sadeghi, F., and Djavanroodi, F. (2008) New analysis for the FGM thick cylinders under combined pressure and temperature loading, American J. of Applied Sci., 5 (7): 852–859.

Aggarwal, B.D., and Broatman, L.J. (1980) Analysis and performance of fibre composites, John Wiley, USA.

Anne, G., Hecht-Mijic, S., Richter, H., Van der Biest, O., and Vleugels, J. (2006) Strength and residual stresses of functionally graded Al2O3/ZrO2 discs prepared by electophoretic deposition, Scripta Materialia, 54: 2053–2056.

Arai, Y., Kobayashi, H., and Tamura, M. (1990) Analysis on residual stress and deformation of functionally gradient materials and its optimum design, Proc. 1st Int. Symposium on FGM, Sendai.

Bhatnagar, N.S., and Gupta, S.K. (1969) Analysis of thick-walled orthotropic cylinder in the theory of creep, J. of Physical Soc. of Japan, 27(6): 1655–1662.

Bhatnagar, N.S., Arya, V.K., and Debonath, K.K. (1980) Creep analysis of orthotropic rotating cylinder, J. of Pressure Vessel Technol., 102: 371– 377.

Bhatnagar, N.S., Kulkarni, P.S., and Arya, V.K. (1986a) Creep analysis of orthotropic rotating cylinder considering finite strains, Int. J. of Non- Linear Mech., 21(1): 61–71.

Bhatnagar, N.S., Kulkarni, P.S., and Arya, V.K. (1986b) Analysis of an orthotropic thick-walled cylinder under primary creep conditions, Int. J. of Pressure Vessels and Piping Tech., 23(3): 165–185.

Bicanic, N., Pearce, C.J., and Owen, D.R.J. (1994) Failure prediction of concrete-like materials using softening Hoffman plasticity model, Proceedings of international conference on computational modeling of concrete structures, EURO-C, 185–198.

Biesheuvel, P. M., and Verweij, H. (2000) Calculation of the composition profile of a functionally graded material produced by centrifugal casting, J. Am. Ceram. Soc., 83: 743–749.

Bonollo, F., Moret, A., Gallo, S., and Mus, C. (2004) Cylinder liners in aluminium matrix composite by centrifugal casting, Materiali Compositi, 6: 49–53.

Bouchafa, A., Benzair, A., Tounsi, A., Draiche, K., Mechab, I., Bedia, E.A.A. (2010) Analytical modeling of thermal residual stresses in exponential functionally graded material system, Materials and Design, 31: 560–563.

Boyle, J.T., and Spence, J. (1983) Stress analysis for creep, London: Butterworth.

Buttlar, W.G., Wagoner, M., You Z., and Brovold, S.T. (2004) Simplifying the hollow cylinders tensile test procedure through volume-based strain, J. of Association of Asphalt Paving Technologies (AAPT), 73: 367–400.

Chen, J.J., Tu, S.T., Xuan, F.Z., and Wang, Z.D. (2007) Creep analysis for a functionally graded cylinder subjected

to internal and external pressure. The J. of Strain Analysis for Engng. Design, 42(2): 69–77.

Chen, W., Gui-ru, Y.E., and Jin-biao, C.A.I. (2002) Themoelastic stresses in a uniformly heated functionally graded isotropic hollow cylinder, J. of Zhejiang University Sci., 3(1): 1–5.

Cho, J. R., and Park, H. J. (2002) High strength, FGM cutting tools: Finite element analysis on thermoelastic characteristics, J. Mater. Process Technol., 130–131: 351–356.

Clyne, T.W., and Withers, P.J. (1993) An introduction to metal matrix composites, Cambridge Univ. Press, Cambridge, U.K., 479: 462–463.

Cooley, W. G., and Palazotto, A. (2005) Finite element analysis of functionally graded shell panels under thermal loading, Proceedings of the 2005 ASME International Congress and Exhibition, Paper No. IMECE 2005–85778.

Crowe, C.R., Gray, R.A., and Hasson, D.F. (1985) Proceedings of 5th International Conference on Composite Materials, San Diago (The Metallurgical Society, Warrendale, Pennsylvania), 843.

Finnie, I. (1960) Steady-state creep of a thick-walled cylinder under combined axial load and internal pressure, J. of Basic Engng., Sep., 689–694.

Fukui, Y., and Yamanaka, N. (1992) Elastic analysis for thick-walled tubes of functionally graded material subjected to internal pressure, JSME Int J. Series I, 35(4): 379–385.

Fukui, Y., Yamanaka, N., and Wakashima, K. (1993) The stresses and strains in a thick-walled tube for functionally graded material under uniform thermal loading, JSME Int. J. Series A, 36(2): 156–162.

Gao, J.W., and Wang C. Y. (2000) Modeling the solidification of functionally graded materials by centrifugal casting, Mater. Sci. and Engng. A, 292: 207–215.

Gonzalez-Doncel, G., and Sherby, O.D. (1993) High temperature creep behaviour of metal matrix aluminium-SiC composites, Acta Metall Mater, 41(10): 2797–2805.

Gupta, S.K., Pathak, S. (2001) Thermo creep transition in a thick walled circular cylinder under internal pressure, Indian J. Pure Appl Math., 32(2): 237–253.

Hagihara, S., and Miyazaki, N. (2008) Finite element analysis for creep failure of coolant pipe in light water reactor due to local heating under severe accident condition, Nuclear Engng Design, 238(1): 33–40.

Han, B.Q., and Langdon, T.G. (2002) Factors contributing to creep strengthening in discontinuously-reinforced materials, Mater. Sci. Engng., A322 (1): 73–78.

Henderson, J., and Snedden, J.D. (1972) Creep fracture of anisotropic cylindrical bars under pure torque, Creep in Structures, ed. J. Hult, Springer-Verlag Berlin, 18.

Hill, R. (1948) Theory of yielding and plastic flow of anisotropic materials. Proc. Roy. Soc. London, A193: 281–297.

Hill, R. (1950) The mathematical theory of plasticity, Oxford, First Ed., Clarendon Press.

Hirai, T. (1996) Functionally gradient materials, Mater Sci. Tech. (Eds. Chan, R.W., Hassen, P. and Cramer, E.J.) VCH, Weinheim, Germany, 17B, 293–341.

Hirai, T. and Chen, L. (1999) Recent and prospective development of functionally graded materials in Japan, Mater. Sci. Forum, 308–311: 509–514.

Hirano, T., and Teraki, J. (1993) Computational approach to design of functionally graded energy conservation materials, in: Modeling and Simulation for Materials Design (Eds. Nishijima, S and Onodera, H.), 303–308.

Librescu, L. and Song, S.Y. (2005) Thin-walled beams made of functionally graded materials and operating in a high temperature environment: Vibration and stability, J. of Thermal Stresses, 28: 649–712.

Liew, K. M., Kitipornchai, S., Zhang, X. Z., and Lim, C. W. (2003) Analysis of the thermal stress behaviour of functionally graded hollow circular cylinders, Int. J. Solids Structures, 40: 2355–2380.

Lim, C. W., and He, L. H. (2001) Exact solution of a compositionally graded piezoelectric layer under uniform stretch, bending and twisting, Int. J. Mech. Sci., 43: 2479–2492.

Liu, Q., Jiao, Y., and Hu, Z. (1996) Theoretical analysis of the particle gradient distribution in centrifugal field during solidification, Metallurgical and Mater. Trans. B, 27B: 1025–1029.

Loghman, A., and Wahab, A. (1996) Creep Damage simulation of thick- walled tubes using the θ projection

concept, Int. J. of Pressure Vessels and Piping, 67(1): 105–111.

Ma, Z.Y., and Tjong, S.C. (1998) Creep behaviour of in-situ Al2O3 and TiB2 particulate mixture-reinforced aluminium composites, Mater. Sci. Engng., A256: 120–128.

Ma, Z.Y., and Tjong, S.C. (2001) Creep deformation characteristics of discontinuously rein forced aluminium-matrix composites, Composites Sci Technol., 61(5): 771–786.

Perry, J., and Aboudi, J. (2003) Elasto-plastic stresses in thick walled cylinders. ASME J. Pressure Vessel Technol., 125(3): 248–252.

Peters, S.T. (1998) Handbook of composites, 2nd Edition. Chapman and Hall, London, UK, 905–956.

Pickel, W., Jr., Sidebowom, O.M., and Boresia, P. (1971) Evaluation of creep laws and flow criteria for two metals subjected to stepped load and temperature changes, Exper. Mechanics, 11(5): 202–209.

Pindera, M.J., Arnold, S.M., Aboudi, J., and Hui, D. (1994) Special Issue: Use of composites in functionally graded materials, Composites Engng., 4: 1–150.

Takezono, S., Tao, K., Inamura, E., and Inoque, M. (1996) Thermal stress and deformation in functionally graded materials shells of revolution under thermal loading due to fluid, JSME Int. J., 39A(4): 573–581.

Tanigawa, Y. (1995) Some basic thermoelastic problems for nonhomogeneous structural materials, Appl. Mech. Rev., 48: 287–300.

Tanigawa, Y., Oka, N., and Akai, T. (1997) One-dimensional transient thermal stress problem for nonhomogeneous hollow circular cylinder and its optimization of material composition for thermal stress relaxation, JSME Int. J. 40A: 117–127.

Tarn, J.Q. (2001) Exact solutions for anisotropic functionally graded cylinders subjected to thermal and mechanical loads, Int. J. of Solids and Structures, 38: 8189–8206.

Tauchert, T.R. (1981) Optimum design of cylindrical pressure vessel, J.of Composite Mater., 15: 390–402.

Taya, M., and Arsenault, R.J. (1989) Metal matrix composites: Thermomechanical behaviour, Pergamon Press, Oxford, UK, 248.

Tzeng, J.T. (1999) Viscoelastic response of composite overwrapped cylinders, J. of Thermoplastic Composite Mater., 12(1): 55–69.

Tzeng, J.T. (2002) Viscoelastic analysis of composite cylinders subjected to rotation, J. of Composite Mater., 36(2): 229–239.

Uemura, S. (2003) The activities of FGM on new applications, Mater. Sci. Forum, 423–425: 1–10.

Williamson, R.L., Rabin, B.N., and Byerly, G.E. (1995) FEM study of the effects of interlayers and creep in reducing residual stresses and strains in ceramic-metal joints, Composites Part B: Engng. 5(7): 851–863.

Yang, Y.Y. (1998) Creep behaviour in a multi-layers joint, Report Forschungszentrum Karlsruhe No. FZKA 6118.

Yang, Y.Y. (1999) Stress analysis in a joint with functionally graded materials considering material creep behaviour, Mater. Sci. Forum, 308-311: 948–954.